
¹¹¹In-Labeled Trastuzumab (Herceptin) Modified with Nuclear Localization Sequences (NLS): An Auger Electron-Emitting Radiotherapeutic Agent for HER2/neu-Amplified Breast Cancer

Danny L. Costantini¹, Conrad Chan¹, Zhongli Cai¹, Katherine A. Vallis², and Raymond M. Reilly^{1,3,4}

¹Departments of Pharmaceutical Sciences, University of Toronto, Toronto, Ontario, Canada; ²Department of Radiation Oncology and Biology, University of Oxford, Oxford, United Kingdom; ³Department of Medical Imaging, University of Toronto, Toronto, Ontario, Canada; and ⁴Toronto General Research Institute, University Health Network, Toronto, Ontario, Canada

The cytotoxicity and tumor-targeting properties of the anti-HER2/neu monoclonal antibody trastuzumab modified with peptides (CGYGPKKKRKVGG) harboring the nuclear localization sequence ([NLS] italicized) of simian virus 40 large T-antigen and radiolabeled with ¹¹¹In were evaluated. **Methods:** Trastuzumab was derivatized with sulfosuccinimidyl-4-(*N*-maleimidomethyl) cyclohexane-1-carboxylate (sulfo-SMCC) for reaction with NLS-peptides and labeled with ¹¹¹In using diethylenetriaminepentaacetic acid (DTPA). The immunoreactivity of ¹¹¹In-NLS-trastuzumab was determined by its ability to displace the binding of trastuzumab to SK-BR-3 human breast cancer (BC) cells. Cellular uptake and nuclear localization were evaluated in SK-BR-3, MDA-MB-361, and MDA-MB-231 BC cells, expressing high, intermediate, or very low levels of HER2/neu, respectively, by cell fractionation and confocal microscopy. Biodistribution and nuclear uptake were compared in athymic mice bearing MDA-MB-361 xenografts. The cytotoxicity of ¹¹¹In-trastuzumab and ¹¹¹In-NLS-trastuzumab was studied by clonogenic assays, and DNA damage was assessed by probing for phosphorylated histone H2AX (γ H2AX) foci. **Results:** The dissociation constant for binding of ¹¹¹In-NLS-trastuzumab to SK-BR-3 cells was reduced <3-fold compared with that of ¹¹¹In-trastuzumab, demonstrating relatively preserved receptor-binding affinity. The receptor-mediated internalization of ¹¹¹In-trastuzumab in SK-BR-3, MDA-MB-361, and MDA-MB-231 cells increased significantly from 7.2% \pm 0.9%, 1.3% \pm 0.1%, and 0.2% \pm 0.05% to 14.4% \pm 1.8%, 6.3% \pm 0.2%, and 0.9% \pm 0.2% for ¹¹¹In-NLS-trastuzumab harboring 6 NLS-peptides, respectively. NLS-trastuzumab localized in the nuclei of BC cells, whereas unmodified trastuzumab remained surface-bound. Conjugation of ¹¹¹In-trastuzumab to NLS-peptides did not affect its tissue biodistribution but promoted specific nuclear uptake in MDA-MB-361 xenografts (2.4–2.9 %ID/g [percentage injected dose per gram] for ¹¹¹In-NLS-trastuzumab and 1.1 %ID/g for ¹¹¹In-trastuzumab). ¹¹¹In-NLS-trastuzumab was 5- and 2-fold more potent at killing SK-BR-3 and MDA-MB-361 cells than ¹¹¹In-trastuzumab, respectively, whereas toxicity toward MDA-

MB-231 cells was minimal. ¹¹¹In-NLS-trastuzumab was 6-fold more effective at killing SK-BR-3 cells than unlabeled trastuzumab. Formation of γ H2AX foci occurred in a greater proportion of BC cells after incubation with ¹¹¹In-NLS-trastuzumab compared with ¹¹¹In-trastuzumab or unlabeled trastuzumab. **Conclusion:** NLS-peptides routed ¹¹¹In-trastuzumab to the nucleus of HER2/neu-positive human BC cells, rendering the radiopharmaceutical lethal to the cells through the emission of nanometer–micrometer range Auger electrons. The greater cytotoxic potency of ¹¹¹In-NLS-trastuzumab compared with unlabeled trastuzumab in vitro and its favorable tumor-targeting properties in vivo suggest that it could be an effective targeted radiotherapeutic agent for HER2/neu-amplified BC in humans.

Key Words: breast cancer; trastuzumab (Herceptin); ¹¹¹In; nuclear translocation; Auger electrons

J Nucl Med 2007; 48:1357–1368
DOI: 10.2967/jnumed.106.037937

The development of recombinant antibodies for cancer therapy has emerged as one of the most promising areas in oncology (1). Trastuzumab (Herceptin; Hoffmann-La Roche), in particular, is a humanized monoclonal antibody (mAb) directed against the human epidermal growth factor receptor-2 (HER2/neu), a transmembrane receptor tyrosine kinase that is overexpressed in 25%–30% of breast cancers (BCs) and distant metastases (2). Trastuzumab shows clinical activity in women with HER2/neu-overexpressing metastatic BC and exhibits synergistic antitumor effects when combined with paclitaxel or anthracyclines, achieving overall response rates of 40%–60% (2). Despite its effectiveness in combination regimens, the response rate to single-agent trastuzumab is only 7%–35%, depending on the level of HER2/neu expression, and the median duration of response is <9 mo (3,4).

Radioimmunotherapy (RIT) may offer the opportunity to enhance the intrinsic cytostatic activity of trastuzumab by incorporating localized radiation directly into the treatment

Received Nov. 7, 2006; revision accepted May 15, 2007.

For correspondence or reprints contact: Raymond M. Reilly, PhD, Leslie Dan Faculty of Pharmacy, University of Toronto, 144 College St., Toronto, Ontario, Canada M5S 3M2.

E-mail: raymond.reilly@utoronto.ca

COPYRIGHT © 2007 by the Society of Nuclear Medicine, Inc.

regimen using the same molecule. Indeed, trastuzumab or its murine mAb analog 4D5, labeled with β -emitters (e.g., ^{131}I , ^{90}Y , or ^{188}Re) (5–7) or α -emitters (e.g., ^{212}Pb , ^{213}Bi , ^{211}At , or ^{225}Ac) (8–11), has been shown to inhibit the growth of HER2/neu-positive human breast, ovarian, nasopharyngeal, prostate, colon, and pancreatic cancer cells in vitro or provide antitumor effects in vivo in xenograft mouse models. For RIT of micrometastatic tumors, however, long-range (2- to 12-mm or 200- to 1,200-cell diameters) β -particle emitters are generally considered suboptimal because a significant portion of the radiation dose is deposited outside the target volume (i.e., in normal tissues surrounding targeted tumor cells) (12). Furthermore, hematologic toxicities are common adverse effects associated with β -particle RIT, primarily due to the prolonged retention time of radiolabeled mAbs in the circulation (half-life [$t_{1/2}$] \sim 6 d) combined with the long range of the β -particles (2–10 mm), which exposes the bone marrow to excessive levels of radiation (1,3). Short-range (40–100 μm) α -particle emitters are theoretically better suited for RIT of micrometastatic disease because a greater fraction of the emitted energy is absorbed by the tumor cells. Their short half-lives (<12 h), however, place constraints on production, antibody labeling, and use, whereas longer-lived α -emitters, such as ^{225}Ac ($t_{1/2}$ = 10 d), are limited by the redistribution of daughter radioisotopes after their decay and consequent irradiation of normal organs (1,13).

Low-energy Auger electron-emitters are an appealing alternative to α - or β -particle emitters for RIT. Most Auger electrons travel nanometer–micrometer distances in tissue and have high linear energy transfer (LET) values approaching those of α -emitters (4–26 keV/ μm) (12). These properties render Auger electron-emitters highly cytotoxic and damaging to DNA when they decay intracellularly, especially when they decay in close proximity to the cell nucleus (14). We recently reported, for example, that the anti-CD33 mAb HuM195, conjugated to the Auger electron-emitter ^{111}In ($t_{1/2}$ = 2.83 d), was toxic to myeloid leukemia cells. Fusion proteins containing a nuclear localization sequence (NLS) have been widely used to exploit intracellular transport mechanisms and promote the translocation of macromolecules into the cell nucleus. NLS-containing macromolecules specifically interact with importin (karyopherin) α - β -transport factors that function as carrier molecules and facilitate the passage of cargo proteins through the nuclear pore complex (15). A single cluster of cationic residues (PKKKRKV) is required for nuclear localization of simian virus 40 (SV40) large T-antigen. This NLS-motif has been conjugated to a variety of macromolecules that are excluded from the nucleus, such as bovine serum albumin, ferritin, IgG, and IgM proteins (15). These proteins undergo efficient nuclear translocation after conjugation to NLS. Therefore, we further modified ^{111}In -HuM195 with 13-mer peptides (CGYGPKKKRVGG) harboring the NLS of SV40 large T-antigen. Conjugation of ^{111}In -HuM195 to NLS-peptides dramatically increased its nuclear uptake in leukemia cells and enhanced its cytotoxicity toward these cells (16). The hypothesis of the current study

was that conjugation of NLS-containing peptides to trastuzumab labeled with the Auger electron-emitter ^{111}In would enhance its toxicity in HER2/neu-positive BC cells in vitro through routing of the radioimmunoconjugates to the cell nucleus. We further hypothesized that the NLS-peptides would not substantially interfere with the receptor-binding affinity of ^{111}In -trastuzumab but would enhance its ability to specifically accumulate into the nucleus of BC cells forming HER2/neu-positive tumor xenografts in athymic mice.

MATERIALS AND METHODS

Cell Culture

SK-BR-3, MDA-MB-361, and MDA-MB-231 human BC cells were obtained from the American Type Culture Collection. SK-BR-3 cells express 2×10^6 HER-2/neu receptors per cell and were cultured in RPMI 1640 with 10% fetal bovine serum (FBS) and 1% penicillin-streptomycin (P/S) (17). In comparison, MDA-MB-361 and MDA-MB-231 cells express 2- and 150-fold lower levels of HER2/neu, respectively, and were maintained in Dulbecco's modified Eagle medium with 10% FBS and 1% P/S (18).

^{111}In -Trastuzumab and ^{111}In -Human IgG Modified with NLS-Peptides

Trastuzumab (Herceptin) or nonspecific, irrelevant human IgG (hIgG; purity \geq 95%, product no. I4506; Sigma-Aldrich) were derivatized with diethylenetriaminepentaacetic acid (DTPA) dianhydride (Sigma-Aldrich) for labeling with ^{111}In (17). Briefly, trastuzumab or hIgG (500 μg , 10 mg/mL) was reacted with a 10-fold molar excess of DTPA for 1 h at room temperature (RT) and then purified on a Sephadex-G50 minicolumn (Sigma-Aldrich) eluted with phosphate-buffered saline (PBS; pH 7.5). Synthetic 13-mer NLS-peptides (CGYGPKKKRVGG) synthesized by the Advanced Protein Technology Centre (Hospital for Sick Children, Toronto, ON) were then conjugated to DTPA-modified trastuzumab or hIgG using the heterobifunctional cross-linking agent sulfosuccinimidyl-4-(*N*-maleimidomethyl)cyclohexane-1-carboxylate (sulfo-SMCC; Pierce) (16). Briefly, DTPA-trastuzumab or hIgG (0.5–2.0 mg, 8 mg/mL in PBS, pH 7.5) was reacted with a 5- to 50-fold molar excess of sulfo-SMCC (2–5 mmol/L) at RT for 1 h, and purified on a Sephadex-G50 minicolumn eluted 20–25 times with 100 μL of PBS (pH 7.0). Fractions 9–14 containing maleimide-derivatized DTPA-trastuzumab or hIgG were pooled and transferred to a Microcon YM-50 ultrafiltration device (Amicon), concentrated to 2–5 mg/mL, and reacted with a 60-fold molar excess of NLS-peptides (5–10 mmol/L in PBS, pH 7.0) overnight at 4°C. DTPA-trastuzumab or hIgG, modified with NLS-peptides (NLS-DTPA-trastuzumab), or NLS-DTPA-hIgG, was purified on a Sephadex-G50 minicolumn eluted with PBS (pH 7.5).

DTPA-trastuzumab, NLS-DTPA-trastuzumab, or NLS-DTPA-hIgG (50–100 μg) was labeled by incubation with 37–111 MBq ^{111}In -acetate for 1 h at RT. ^{111}In -Acetate was prepared by mixing ^{111}In -chloride (MDS-Nordion, Inc.) with 1.0 mol/L sodium acetate (pH 6.0 [1:1, v/v]). After purification on a Sephadex-G50 minicolumn, radiochemical purity was routinely $>97\%$ as determined by instant thin-layer silica-gel chromatography (ITLC-SG; Pall Corp.) developed in 100 mmol/L sodium citrate (pH 5.0) (R_f : ^{111}In -labeled immunoconjugates, 0.0; free ^{111}In -DTPA, 1.0). Radioactivity measurements were made using an automatic γ -counter (Wallac Wizard-1480; Perkin Elmer).

Characterization of DTPA-Trastuzumab Modified with NLS-Peptides

The purity and homogeneity of NLS-DTPA-trastuzumab immunoconjugates were evaluated by sodium dodecyl sulfonate–polyacrylamide gel electrophoresis (SDS–PAGE) on a 5% Tris–HCl minigel (Bio-Rad) electrophoresed under nonreducing conditions and by Western blot. The gel was stained with Coomassie-G250 stain (Bio-Rad). For the Western blot, electrophoresed proteins were transferred onto polyvinylidene difluoride membranes (Roche) and incubated in 5% skim milk in PBS/0.1% Tween-20 (PBS-T) for 1 h at RT, followed by an overnight incubation at 4°C with horseradish peroxidase–conjugated goat-antihuman Fc antibodies (1:1,500; Sigma-Aldrich). After 3 washes with PBS-T, reactive bands were detected using the chromogenic substrate 3,3'-diaminobenzidine tetrahydrochloride (Sigma-Aldrich) and 0.03% H₂O₂. The migration distance of the reactive bands relative to the front (R_f) was measured, and the logarithm of molecular weight (M_r) versus $1/R_f$ was plotted by comparison with standard M_r reference markers (10–250 kDa; Amersham Biosciences) electrophoresed under identical conditions. To determine the number of NLS-peptides conjugated to DTPA-trastuzumab, the difference between the M_r values for DTPA-trastuzumab and NLS-DTPA-trastuzumab was divided by the M_r of the NLS-peptide (~1,418 Da). Alternatively, the number of NLS-peptides incorporated into trastuzumab was quantified by including a tracer amount of ¹²⁵I-labeled NLS-peptides in the reaction, measuring the proportion of bound radioactivity after purification, and multiplying by the peptides-to-trastuzumab molar ratio used in the reaction (16). NLS-peptides were radiolabeled to a specific activity of 2–5 MBq/mg with ¹²⁵I-sodium iodide (MDS-Nordion, Inc.) using the IODO-GEN method (Pierce) (16). The radiochemical purity of ¹²⁵I-NLS-peptides was >95% as determined by paper chromatography developed in 85% methanol (R_f : ¹²⁵I-NLS-peptides, 0.0; ¹²⁵I iodide, 1.0).

Competition Receptor-Binding Assays

Approximately 5×10^4 SK-BR-3 cells were incubated in 96-well plates for 24 h in culture medium. After a gentle rinse with PBS (pH 7.5), the cells were incubated with ¹¹¹In-NLS-trastuzumab or ¹¹¹In-trastuzumab (10 nmol/L), in the presence of unlabeled trastuzumab (0–300 nmol/L) in 100 μ L PBS (pH 7.5) containing 0.1% bovine serum albumin (BSA) 4°C. The cells were rinsed with PBS (pH 7.5) and solubilized in 100 mmol/L NaOH. Cell suspensions were collected and the radioactivity was measured in a γ -counter. The proportion of ¹¹¹In-trastuzumab/¹¹¹In-NLS-trastuzumab displaced from SK-BR-3 cells by increasing concentrations of trastuzumab was plotted, and Origin version 6.0 (Microcal Software, Inc) was used to fit the curves and determine the dissociation constants (K_d).

Radioligand Internalization Studies

Approximately 1×10^6 cells were incubated at 37°C with agitation in microtubes containing ¹¹¹In-trastuzumab or ¹¹¹In-NLS-trastuzumab (10 nmol/L) in 500 μ L PBS (pH 7.5) with 0.1% BSA. At selected time points up to 24 h, the cells were centrifuged and the medium was removed. Cells were washed twice with PBS (pH 7.5) to remove unbound radioactivity and resuspended in a 0.5-mL mixture of 200 mmol/L sodium acetate and 500 mmol/L sodium chloride (pH 2.5) for 5 min on ice (19). Cells were then centrifuged again to separate internalized-radioactivity (pellet) from surface-bound radioactivity present in the acid wash (supernatant). After 2 more washes with PBS (pH 7.5), the pellets and supernatants were measured in a γ -counter.

Confocal Immunofluorescence Microscopy

Cells were cultured on chamber-slides (Nunc; Life Technologies) overnight at 37°C in medium. To assess the subcellular distribution of trastuzumab, cells were incubated with DTPA-trastuzumab or NLS-DTPA-trastuzumab (1.5 μ g/mL) in 1 mL of medium for 24 h at 37°C. Cells were then fixed with 3.7% paraformaldehyde and permeabilized for 10 min with PBS (pH 7.5) containing 0.1% Triton X-100, 1% BSA, and 2% goat serum. After three 10-min washes with PBS (pH 7.5), the slides were blocked for 2 h with 10% goat serum and incubated with AlexaFluor-594 antihuman IgG (Molecular Probes).

An early step in the response of cells to DNA double-strand breaks (DSBs) after exposure to ionizing radiation is the phosphorylation of histone-H2AX at serine-139 (γ H2AX), which can be detected as discrete nuclear foci using γ H2AX-specific antibodies (20). The ability of ¹¹¹In-trastuzumab and ¹¹¹In-NLS-trastuzumab to cause DNA DSBs in BC cells was evaluated using this γ H2AX assay. Briefly, cells were cultured overnight in 1 mL of medium containing PBS (pH 7.5), trastuzumab, ¹¹¹In-trastuzumab, or ¹¹¹In-NLS-trastuzumab (67.5 μ g/mL, 19.8 MBq) and then fixed with 2% paraformaldehyde containing 0.5% Triton X-100 in PBS (pH 8.2) for 15 min. After three 10-min washes with PBS (pH 7.5) containing 0.5% BSA and 0.2% Tween-20, the cells were permeabilized for 15 min with PBS (pH 8.2) containing 0.5% Nonidet P-40 and blocked for 1 h in 2% BSA and 1% donkey serum. The slides were then incubated with antiphospho- γ H2AX (1:800; Upstate Biotechnology) in 3% BSA overnight at 4°C and then AlexaFluor-488 antimouse IgG (Molecular Probes) for 45 min at RT.

All slides were mounted with Vectashield mounting media containing 4,6-diamidino-2-phenylindole (DAPI) (Vector Laboratories) and kept at 4°C overnight. Images were taken with an inverted LSM510 confocal microscope (Carl Zeiss) at the Advanced Optical Microscopy Facility (Princess Margaret Hospital, Toronto, Ontario, Canada). Excitation was at 364, 488, or 543 nm for visualization of DAPI, AlexaFluor-488, or AlexaFluor-594, using 385- to 470-nm, 505- to 550-nm, or 560-nm emission filters, respectively. For imaging of γ H2AX, 10–15 Z-stack images at 1.2- μ m intervals were acquired throughout the entire cell nucleus, merged using LSM-Viewer software (version 3.5.0.376; Zeiss), and stored as tiff files. The number of γ H2AX foci present in each cell was counted manually using ImageJ software (version 1.36b; National Institutes of Health), and cells with >10 foci per nucleus were classified as positive for radiation-induced γ H2AX (20).

Clonogenic Assays

Approximately 2×10^6 cells were incubated with ¹¹¹In-trastuzumab (244 \pm 22 MBq/mg) or ¹¹¹In-NLS-trastuzumab (239 \pm 8.9 MBq/mg) in 1 mL of medium in microtubes for 24 h at 37°C. Controls included cells cultured with medium alone, medium containing unlabeled trastuzumab, or medium containing ¹¹¹In-NLS-hIgG–nonspecific, irrelevant immunoconjugates (228 \pm 13 MBq/mg). Cells were then centrifuged at 1,000g for 5 min and washed twice with medium. Sufficient cells were then plated in triplicate in 12-well plates and cultured in medium at 37°C. After 14–21 d, colonies of ≥ 50 cells (or ≥ 0.2 mm for MDA-MB-361 cells) were stained with methylene blue and counted. The surviving fraction (SF) was calculated by dividing the number of colonies formed for treated cells by the number for untreated cells. Survival curves were derived by plotting the SF values versus the concentration (μ g/mL) of antibody used.

Tumor and Normal Tissue Biodistribution Studies

The tissue biodistribution of ^{111}In -trastuzumab, ^{111}In -NLS-trastuzumab, and nonspecific, irrelevant ^{111}In -NLS-hIgG control immunoconjugates was evaluated in athymic mice implanted subcutaneously with MDA-MB-361 BC xenografts. Mice were implanted intradermally with a 17- β -estradiol pellet (Innovative Research of America) 24 h before inoculation in the flank with 1×10^7 MDA-MB-361 cells in 100 μL of Matrigel (Becton-Dickinson Labware) and culture medium mixture (1:1, v/v). When the tumors reached a diameter of 2–5 mm (6–8 wk), the mice received an intravenous injection of ^{111}In -trastuzumab, ^{111}In -NLS-trastuzumab, or ^{111}In -NLS-hIgG (10 μg ; 1–2 MBq). At 72 h after injection, the mice were sacrificed and a blood sample was taken by intracardiac puncture. The tumor and samples of selected normal tissues were removed, blotted dry, and weighed. Uptake of radioactivity by these tissues was measured in a γ -counter and expressed as the percentage injected dose per gram (%ID/g) and as the tumor-to-normal tissue ratios. The principles of *Laboratory Animal Care* (NIH Publication no. 86-23, revised 1985 [Bethesda, MD]) were followed, and animal studies were approved by the Animal Care Committee at the University Health Network (Protocol no. TG:282.2) following Canadian Council on Animal Care guidelines.

Nuclear Uptake In Vivo in Tumors and Normal Tissues

The accumulation of radioactivity in the nuclei of BC cells, as well as in cells of selected normal tissues (liver, kidney, spleen, and heart), was determined by subcellular fractionation after intravenous injection (10 μg ; 1–2 MBq) of ^{111}In -trastuzumab, ^{111}In -NLS-trastuzumab, or ^{111}In -NLS-hIgG—nonspecific, irrelevant control immunoconjugates in athymic mice bearing subcutaneous MDA-MB-361 tumor xenografts. At 72 h after injection, groups of 3 mice were sacrificed and tissue samples were taken to measure the tissue radioactivity concentration (%ID/g). The nuclei were separated from the cytoplasm/membrane using the Nuclei PURE Prep Nuclei Isolation Kit (Sigma-Aldrich) following the manufacturer's directions. We previously demonstrated (21) by Western blot for calpain, an abundant cytoplasmic protein and p84, a nuclear matrix protein (unpublished results), that this method provides a highly pure nuclear and cytoplasm/membrane fraction. Nuclear uptake was quantified by multiplying the %ID/g values by the percentage of radioactivity present in the nuclear fraction.

Statistical Methods

Data are presented as mean \pm SEM. Statistical comparisons were made using the Student *t* test. For the γH2AX study, a χ^2 analysis was used to evaluate differences between treatment groups. $P < 0.05$ was considered significant.

RESULTS

Characterization of NLS-Trastuzumab Immunoconjugates

As determined by SDS-PAGE and Western blot, the M_r for trastuzumab IgG increased from 159 ± 2.0 to 178 ± 3.6 kDa as the SMCC-to-trastuzumab molar ratio increased, indicating incremental conjugation to 13-mer peptides (CGYGPKKKRVGG) harboring the NLS of SV40 large-T antigen (Figs. 1A and 1B). According to these M_r values, approximately 1.6 ± 0.3 , 3.4 ± 0.2 , 6.3 ± 0.2 , and 10.4 ± 0.8 NLS-peptides were conjugated to trastuzumab

at an SMCC-to-IgG molar ratio of 5:1, 15:1, 25:1, and 50:1, respectively. Higher molecular-weight dimer and polymer IgG complexes were also observed, likely due to the bicyclic nature of DTPA-dianhydride (22). The proportion of polymeric forms was not significantly different for DTPA-trastuzumab modified with 3 or 6 NLS-peptides ($14.2\% \pm 5.9\%$ and $14.9\% \pm 3.9\%$) than for unmodified DTPA-trastuzumab ($14.9\% \pm 5.4\%$; $P > 0.05$). There was an excellent correlation ($r^2 = 0.99$) between the number of NLS-peptides introduced into trastuzumab determined by M_r analysis or by measuring the proportion of tracer ^{123}I -NLS-peptides incorporated. Indeed, the ^{123}I -NLS-peptide coupling efficiency increased from $4.4\% \pm 0.3\%$ to $9.8\% \pm 0.4\%$ for an SMCC-to-IgG ratio of 15:1 to 25:1, respectively, to $14.8\% \pm 0.7\%$ at a ratio of 50:1 (Figs. 1C and 1D). Thus, a 60-fold molar excess of ^{123}I -NLS-peptides used in the reaction represents 2.5 ± 0.3 , 5.6 ± 0.5 , and 8.4 ± 0.9 incorporated peptides at a 15:1, 25:1, and 50:1 molar ratio, respectively.

Immunoreactivity of ^{111}In -Trastuzumab and ^{111}In -NLS-Trastuzumab

In competition receptor-binding assays, ^{111}In -trastuzumab and ^{111}In -NLS-trastuzumab were displaced by increasing amounts of unlabeled trastuzumab (Fig. 2). Although specific binding to HER2/neu-overexpressing SK-BR-3 cells was found, there was a 1.4-fold and 2.6-fold significant decrease in the receptor-binding affinity for ^{111}In -NLS-trastuzumab bearing 3 (^{111}In -NLS₃-trastuzumab) and 6 (^{111}In -NLS₆-trastuzumab) NLS-peptides ($K_d = 5.9 \pm 0.4$ nmol/L and 3.1 ± 0.4 nmol/L, respectively) compared with ^{111}In -trastuzumab ($K_d = 8.2 \pm 0.5$ nmol/L).

Internalization and Nuclear Translocation of ^{111}In -NLS-Trastuzumab

The internalization of ^{111}In -trastuzumab and ^{111}In -NLS-trastuzumab were compared in SK-BR-3, MDA-MB-361, and MDA-MB-231 cells expressing high, intermediate, or very low levels of HER2/neu, respectively. The fraction of radioactivity that internalized in SK-BR-3 cells, with respect to the total amount of ^{111}In -NLS₃-trastuzumab or ^{111}In -NLS₆-trastuzumab that was added to the incubation media, increased from $7.3\% \pm 2.3\%$ and $5.7\% \pm 1.5\%$ after 2 h of incubation to $11.6\% \pm 1.9\%$ and $14.4\% \pm 1.8\%$ after 24 h, respectively (Fig. 3A). Conversely, the fraction of radioactivity that internalized in SK-BR-3 cells for ^{111}In -trastuzumab reached a plateau at 12 h and decreased after 24 h to $7.2\% \pm 0.9\%$. The uptake of radioactivity was almost completely blocked by the addition of unlabeled trastuzumab to the incubation media, thus demonstrating the specificity for HER2/neu. The uptake of radioactivity in MDA-MB-361 and MDA-MB-231 cells, with respect to the total amount of ^{111}In -NLS-trastuzumab or ^{111}In -trastuzumab added to the incubation media, was significantly lower at 24 h compared with that of SK-BR-3 cells (Figs. 3B and 3C); however, conjugation to NLS-peptides markedly enhanced the fraction of radioactivity that accumulated in these cells

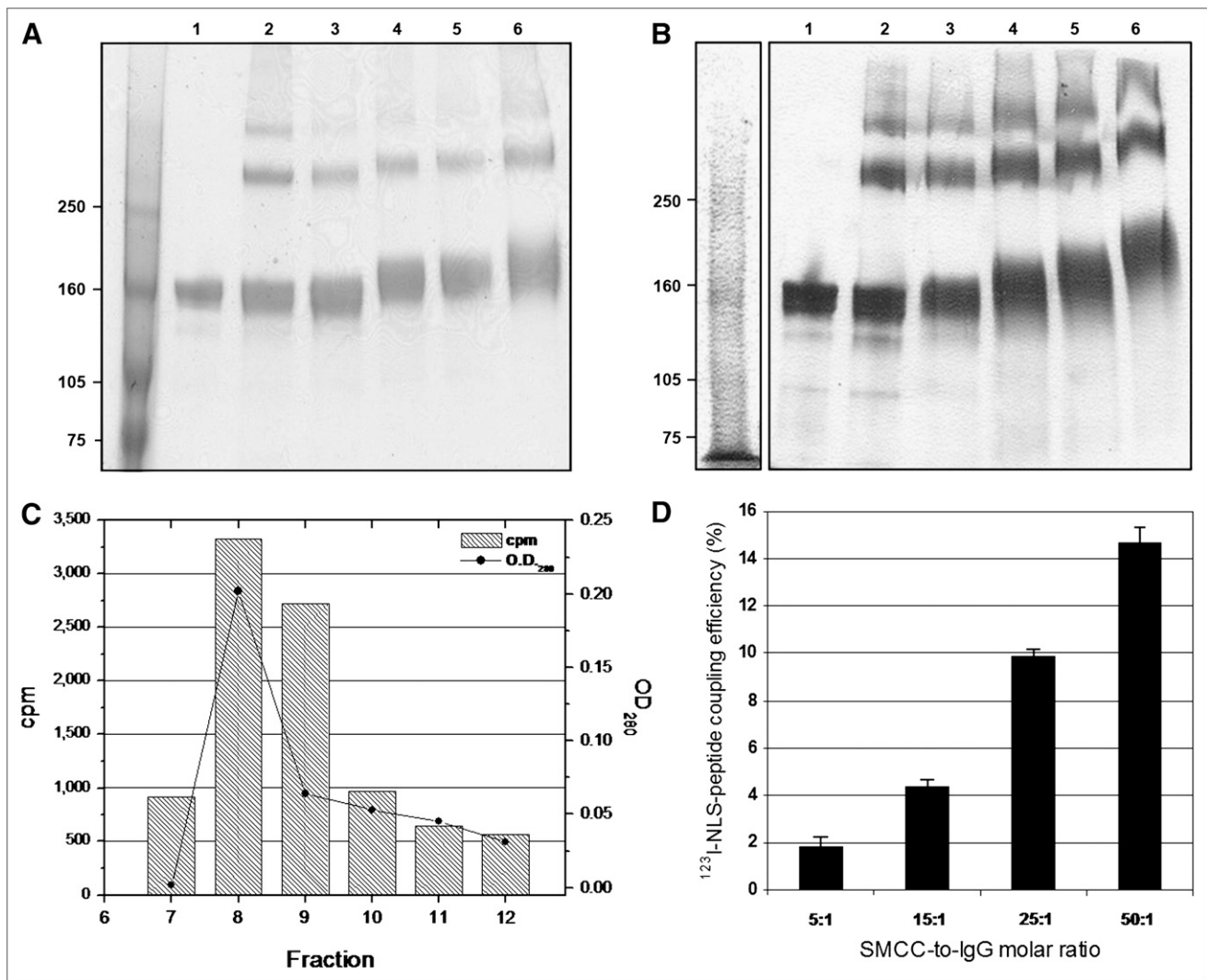


FIGURE 1. (A) SDS-PAGE and (B) Western blot of unmodified trastuzumab (lane 1) or DTPA-trastuzumab (lane 2) reacted with a 5-, 15-, 25-, or 50-fold molar excess of sulfo-SMCC followed by conjugation to a 60-fold molar excess of NLS-peptides (lanes 3–6, respectively). The y-axis indicates M_r (kDa). (C) Representative size-exclusion chromatograms of purification of ^{125}I -NLS-peptides bound to trastuzumab from free peptides. Elution curves were obtained by measuring ultraviolet absorbance ($\text{OD}_{280\text{nm}}$) (solid line) and radioactivity (hatched bars) in each fraction. The peak in fractions 7–10 represents trastuzumab-bound ^{125}I -NLS-peptides. (D) ^{125}I -NLS-peptide coupling efficiency to trastuzumab increases as the SMCC-to-IgG molar ratio increases. Values shown are mean \pm SEM of triplicate determinations.

after incubation with ^{111}In -trastuzumab. Figure 3D shows the internalized fractions, with respect to the total cell-bound radioactivity that was associated with each cell line. These were all significantly greater after incubation with ^{111}In -NLS₃-trastuzumab and ^{111}In -NLS₆-trastuzumab, compared with ^{111}In -trastuzumab. The remaining fraction of radioactivity that was removed in the acid wash was considered to be membrane-bound.

After incubation with DTPA-trastuzumab or DTPA-NLS-trastuzumab, SK-BR-3, MDA-MB-361, and MDA-MB-231 cells were fixed and permeabilized before incubation with fluorophore-conjugated secondary antibodies specific for human IgG. As shown in Figures 4A and 4B, the nucleus and plasma membrane of MDA-MB-361 and SK-BR-3 cells demonstrated moderate to strong immunofluorescence

after incubation with NLS-DTPA-trastuzumab, whereas the signal was restricted to the plasma membrane in cells treated with DTPA-trastuzumab. In contrast, the fluorescence signal was not detected in HER2/neu-negative MDA-MB-231 cells after incubation with DTPA-trastuzumab or NLS-DTPA-trastuzumab (Fig. 4C) or in SK-BR-3 cells incubated without trastuzumab (data not shown), thus demonstrating the specificity of the interactions.

Cytotoxicity of ^{111}In -NLS-Trastuzumab and DNA Damage in BC Cells

There was a dose-dependent effect on the clonogenic survival of SK-BR-3 cells treated with ^{111}In -NLS₃-trastuzumab or ^{111}In -NLS₆-trastuzumab, and the survival was significantly reduced to $24.0\% \pm 4.7\%$ and $10.5\% \pm 2.1\%$,

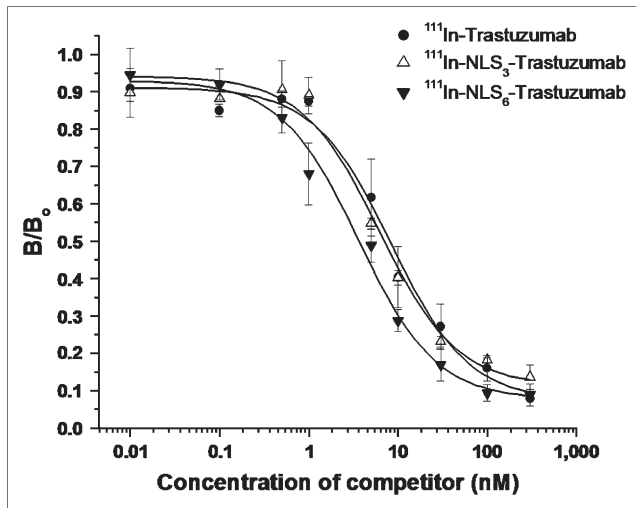


FIGURE 2. Competition binding curve shows effect of increasing concentrations of unlabeled trastuzumab on the displacement of binding of ^{111}In -Trastuzumab or ^{111}In -NLS-Trastuzumab to SK-BR-3 cells. B = radioligand bound in presence of competitors; B_0 = radioligand bound without competitor. Each point represents mean \pm SEM of 3 assays performed in triplicate.

respectively, at the highest concentration tested, whereas ^{111}In -trastuzumab and unlabeled trastuzumab reduced the survival to $52.7\% \pm 3.0\%$ and $64.6\% \pm 3.0\%$, respectively (Fig. 5A). There was no significant toxicity toward SK-BR-3 cells after treatment with nonspecific, irrelevant ^{111}In -NLS-hIgG control immunoconjugates. MDA-MB-361 cells were less sensitive to the cytotoxic effects of ^{111}In -NLS-trastuzumab; however, their clonogenic survival was similarly reduced in a dose-dependent fashion to $40.3\% \pm 7.6\%$ and $26.6\% \pm 6.7\%$ when treated at the highest concentration of ^{111}In -NLS₃-trastuzumab or ^{111}In -NLS₆-trastuzumab, respectively (Fig. 5B). Modest killing of MDA-MB-361 cells was obtained with ^{111}In -trastuzumab without NLS-peptides and unlabeled trastuzumab; at similar concentrations, the survival of MDA-MB-361 cells was reduced to $66.0\% \pm 3.4\%$ and $83.7\% \pm 1.8\%$, respectively. Conversely, ^{111}In -trastuzumab and ^{111}In -NLS-trastuzumab demonstrated only weak cytotoxicity toward HER2/neu-negative MDA-MB-231 cells (Fig. 5C).

As shown in Figures 5D–5G, the percentage of γH2AX -positive SK-BR-3 and MDA-MB-361 cells increased significantly from 45% and 68% after treatment with ^{111}In -trastuzumab to 67% and 84% after treatment with ^{111}In -NLS-trastuzumab, respectively (χ^2 analysis, $P < 0.05$). In contrast, the proportion of γH2AX -positive trastuzumab-treated SK-BR-3 or MDA-MB-361 cells was not significantly different than that of PBS-treated controls. Less than 10% of MDA-MB-231 cells exposed to any of the treatments were γH2AX -positive.

Biodistribution and Nuclear Importation of ^{111}In -NLS-Trastuzumab in BC Xenografts and Normal Tissues

Tumor uptake in athymic mice bearing subcutaneous HER2/neu-positive MDA-MB-361 BC xenografts at 72 h after

injection was relatively high and ranged from $13.2 \pm 2.2\% \text{ID/g}$ for ^{111}In -trastuzumab to 12.1 ± 1.3 and $12.6 \pm 0.4\% \text{ID/g}$ for ^{111}In -NLS₃-trastuzumab and ^{111}In -NLS₆-trastuzumab, respectively ($P > 0.05$; Table 1). Tumor-to-blood ratios were 6.04 ± 0.8 and 5.7 ± 0.7 for ^{111}In -NLS₃-trastuzumab and ^{111}In -NLS₆-trastuzumab, respectively, compared with 6.6 ± 1.1 for ^{111}In -trastuzumab. The highest concentration of radioactivity in normal tissues was found in liver, kidneys, and spleen. In contrast, tumor uptake of ^{111}In -NLS-hIgG—nonspecific, irrelevant control immunoconjugates was significantly lower than that for ^{111}In -NLS-trastuzumab ($4.8 \pm 0.8\% \text{ID/g}$), and the tumor-to-blood ratio was only 1.7 ± 0.4 , indicating that ^{111}In -NLS-trastuzumab specifically targeted HER2/neu-positive tumors in athymic mice.

Radioactivity that accumulated in the nuclei of tumor cells, as well as cells of selected normal tissues (liver, kidneys, spleen, and heart), in athymic mice bearing subcutaneous MDA-MB-361 xenografts at 72 h after injection of ^{111}In -trastuzumab or ^{111}In -NLS-trastuzumab are shown in Table 2. The percentage of radioactivity associated with the nuclei of MDA-MB-361 cells for ^{111}In -NLS₃-trastuzumab and ^{111}In -NLS₆-trastuzumab was significantly higher than that for ^{111}In -trastuzumab or ^{111}In -NLS-hIgG. Conversely, the percentage of radioactivity in the nuclei of cells in liver, spleen, kidney, or heart was not significantly different for any of the ^{111}In -labeled antibodies. On a per-gram basis, approximately 20% of the radioactivity that accumulated in MDA-MB-361 tumor xenografts for ^{111}In -NLS-trastuzumab was present in the nuclear fraction.

DISCUSSION

The results of this study demonstrated that synthetic 13-mer peptides (CGYGPKKKRKKVGG) harboring the NLS of SV40 large-T antigen facilitated the translocation of ^{111}In -trastuzumab into the nucleus of HER2/neu-overexpressing BC cells, where the cytotoxicity of the emitted Auger electrons was enhanced. Furthermore, the dose-dependent cytotoxicity of ^{111}In -NLS-trastuzumab against BC cells was shown to be specific and directly correlated with the cell-surface expression level of HER2/neu. In the clinical setting, metastatic BC patients are selected for treatment with trastuzumab only if the primary tumor demonstrates significantly amplified HER2/neu expression (i.e., Herceptest or other immunohistochemical score of 3+ or moderate–high levels of gene amplification by fluorescence in situ hybridization [FISH]); these patients exhibit a better response than those with lower gene copy number by FISH or intermediate-staining tumors (i.e., Herceptest score $\leq 2+$) (4,23). Nevertheless, those patients who show an initial response to trastuzumab often acquire resistance to the drug in less than a year (24). The dramatically enhanced cytotoxic effects of ^{111}In -NLS-trastuzumab compared with unlabeled trastuzumab found in this study—if translated into in vivo antitumor effects—suggest that this radiotherapeutic agent could potentially offer a more effective treatment for HER2/neu-positive metastatic BC.

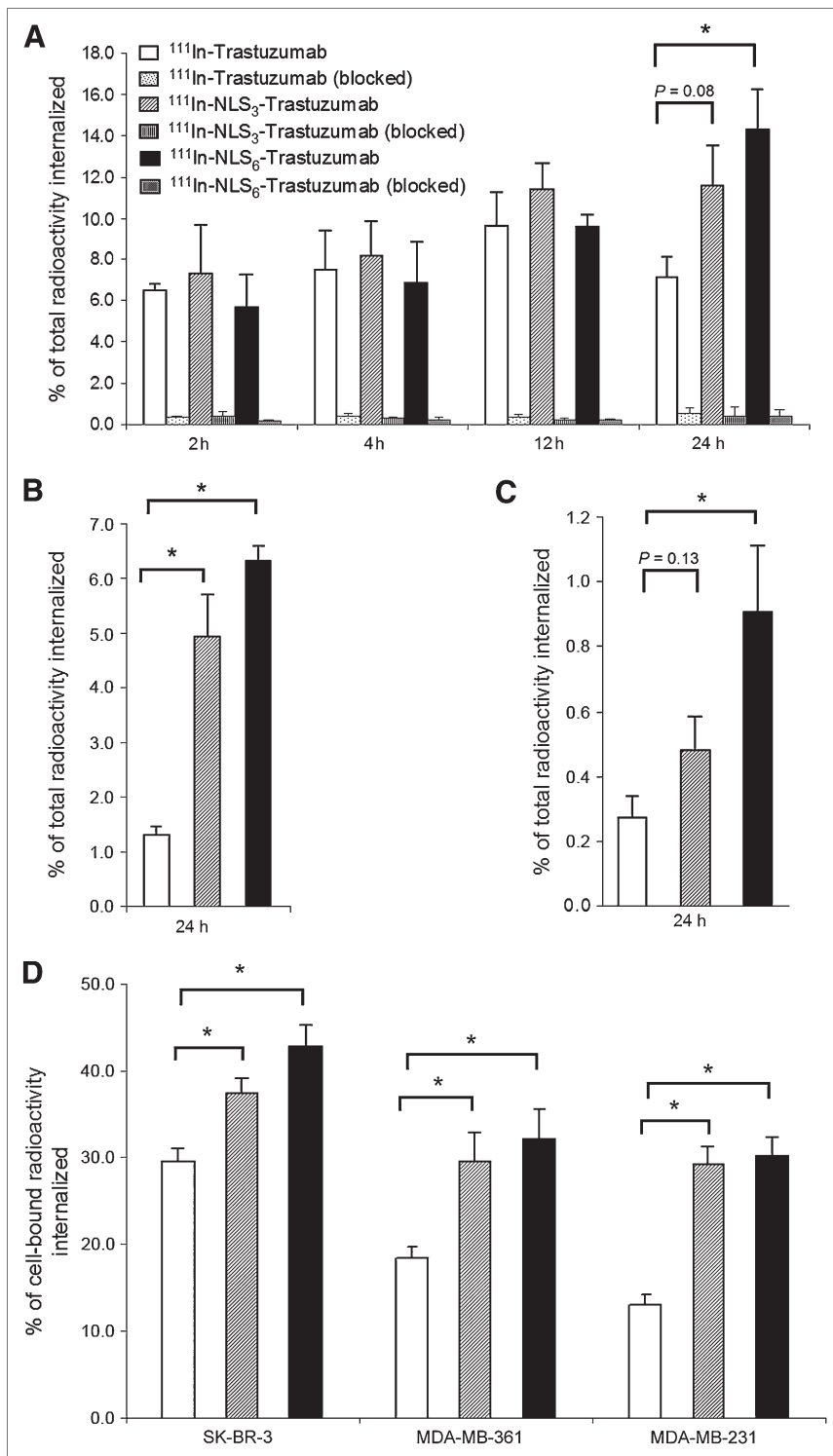


FIGURE 3. Internalization of ^{111}In -NLS-Trastuzumab and ^{111}In -Trastuzumab by SK-BR-3 (A), MDA-MB-361 (B), and MDA-MB-231 (C) BC cells (solid bars) with respect to the total amount of radioactivity added to incubation media. Internalization was measured in presence or absence of an excess of unlabeled trastuzumab (100 nmol/L) in incubation medium to block HER2/neu receptors. (D) Internalized fraction of cell-bound radioactivity. Values shown are mean \pm SEM of triplicate determinations. * $P < 0.05$.

^{111}In -Labeled 4D5 and 21.1 murine mAbs specific for HER2/neu have been found previously to be effective for killing SK-BR-3 breast and SK-OV-3.ip1 ovarian carcinoma cells, either alone or in combination (25). We anticipated that the cytotoxic effects of ^{111}In -trastuzumab (humanized version of 4D5) would be equally as effective as its ^{111}In -labeled 4D5 murine counterpart. At the specific ac-

tivities used in our study (~ 240 MBq/mg), ^{111}In -trastuzumab only demonstrated a 1.2-fold increase in toxicity compared with unlabeled trastuzumab (Fig. 5). Nearly 99% of the low-energy Auger electrons emitted by ^{111}In have a range of $< 1 \mu\text{m}$ in tissues (26), and the radiation-absorbed dose to the nucleus is 2-fold and 35-fold greater when ^{111}In decays in the nucleus compared with when the decay occurs in the

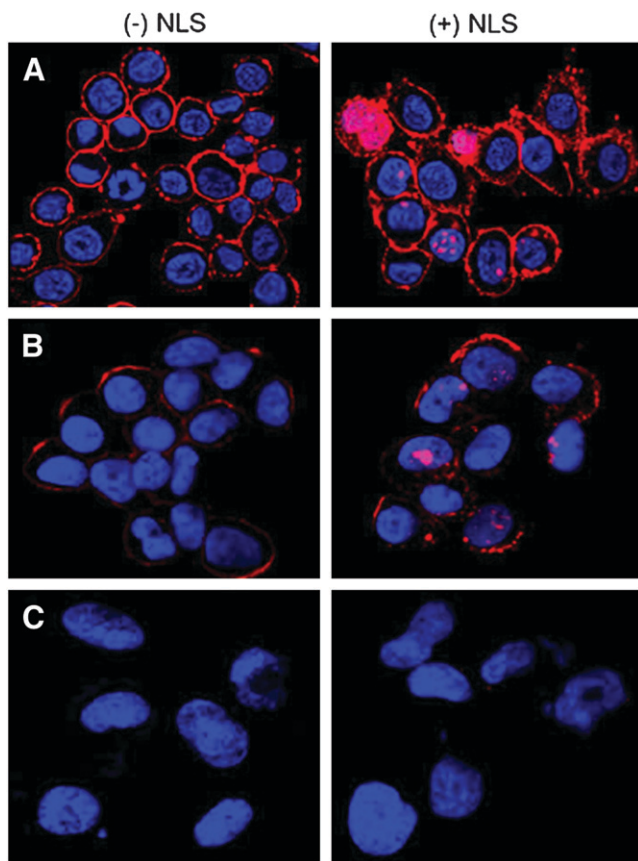


FIGURE 4. Confocal immunofluorescence microscopy of SK-BR-3 (A), MDA-MB-361 (B), and MDA-MB-231 (C) BC cells incubated with DTPA-trastuzumab with (+) or without (-) NLS-peptides. Trastuzumab was detected using an AlexaFluor-564 antihuman IgG secondary antibody (red), and the nucleus was visualized with DAPI (blue). Merging of the 2 signals is shown and images are 1- μ m slices through the cells.

cytoplasm or on the cell surface, respectively (19). Therefore, we further modified ^{111}In -trastuzumab with NLS-peptides to enhance its radiotoxicity through promoting its nuclear uptake after receptor-mediated endocytosis. Indeed, ^{111}In -NLS-trastuzumab substituted with 6 NLS-peptides was approximately 2-fold and 5-fold more potent at killing MDA-MB-361 and SK-BR-3 cells, respectively, compared with ^{111}In -trastuzumab and nearly 3-fold and 6-fold more effective than unlabeled trastuzumab, respectively (Fig. 5). Moreover, the increased sensitivity to cell killing correlated with an increase in γH2AX foci in MDA-MB-361 and SK-BR-3 cells after exposure to ^{111}In -trastuzumab (1.3- and 3.5-fold increase, respectively) and ^{111}In -NLS-trastuzumab (1.6- and 5.2-fold increase, respectively), illustrating the effects of subcellular distribution in determining the biologic impact of Auger electron emitters (14,19). Unexpectedly, MDA-MB-361 cells demonstrated substantial basal levels of γH2AX foci; these findings may be explained by a mutation in p53 in these cells that could result in an inability to respond appropriately to DNA strand breaks (27). Less than 10% of

MDA-MB-231 cells were killed after exposure to ^{111}In -NLS-trastuzumab, suggesting that the toxicity of the radiopharmaceutical was HER2/neu-selective.

After incubation with ^{111}In -trastuzumab or ^{111}In -NLS-trastuzumab, 55%–80% of the radioactivity associated with HER2/neu-positive BC cells remained surface-bound (Fig. 3D), which was consistent with the robust membrane immunofluorescence that was visualized on these cells after incubation with these antibodies (Fig. 4). These findings are in agreement with previous observations that HER2/neu-bound trastuzumab is predominantly surface-localized and is slowly taken up into SK-BR-3 cells with an internalization half-life of approximately 19 h (28). However, the NLS of SV40 large T-antigen (15) was nevertheless able to mediate the translocation of covalently linked ^{111}In -trastuzumab molecules into the nuclei of HER2/neu-expressing BC cells after their receptor-mediated-internalization (Fig. 4; Table 2). Other NLS-containing bioconjugates labeled with Auger electron-emitting radionuclides have been described. For example, we recently reported that NLS-peptide modification of ^{111}In -HuM195 mAb, specific for CD33-epitopes, promoted its nuclear translocation in HL-60 leukemic cells and was 12-fold more radiotoxic than unmodified ^{111}In -HuM195 (16). Similarly, NLS-peptides promoted the translocation of radioactivity into the nucleus of human embryonic kidney (HEK-293) cells (transfected with the somatostatin receptor-2A [SSTR_{2A}]) when incubated with an ^{111}In -labeled somatostatin-based analog (29). NLS-peptides have also been shown to promote the translocation of a [$^{99\text{m}}\text{Tc}(\text{OH})_2(\text{CO})_3$] $^+$ -labeled DNA-intercalating pyrene moiety into the nuclei of B16F1 mouse melanoma cells, where the Auger electrons from $^{99\text{m}}\text{Tc}$ were lethal (30). Taken together, these studies demonstrate that bioconjugates internalized into tumor cells through receptor-mediated processes can be efficiently routed to the nucleus through their modification with NLS-containing peptides and that this strategy can be exploited for targeted radiotherapy of hematologic as well as solid tumors using nanometer–micrometer range Auger electron emitters.

The NLS-peptides mediated nuclear translocation of ^{111}In -trastuzumab but it was critical to preserve HER2/neu receptor binding to permit internalization into BC cells in vitro as well as to target these radiopharmaceuticals to HER2/neu-positive tumors in vivo. Despite the minor (<3-fold) decrease in HER2/neu receptor-binding affinity (Fig. 2), the magnitude of internalization of ^{111}In -NLS-trastuzumab into SK-BR-3, MDA-MB-361, and MDA-MB-231 cells was correlated with their relative expression of HER2/neu (Fig. 3). It should be noted, however, that the internalization values are possibly underestimates, as it has been shown that exposure of cells to low pH buffers to remove surface-bound radioligands may remove some internalized radioactivity (31). Nevertheless, the internalization of ^{111}In -NLS-trastuzumab was significantly higher than the uptake of ^{111}In -trastuzumab without NLS-peptides. As discussed previously, NLS-peptides mediate nuclear importation of internalized molecules, but the mechanism of this

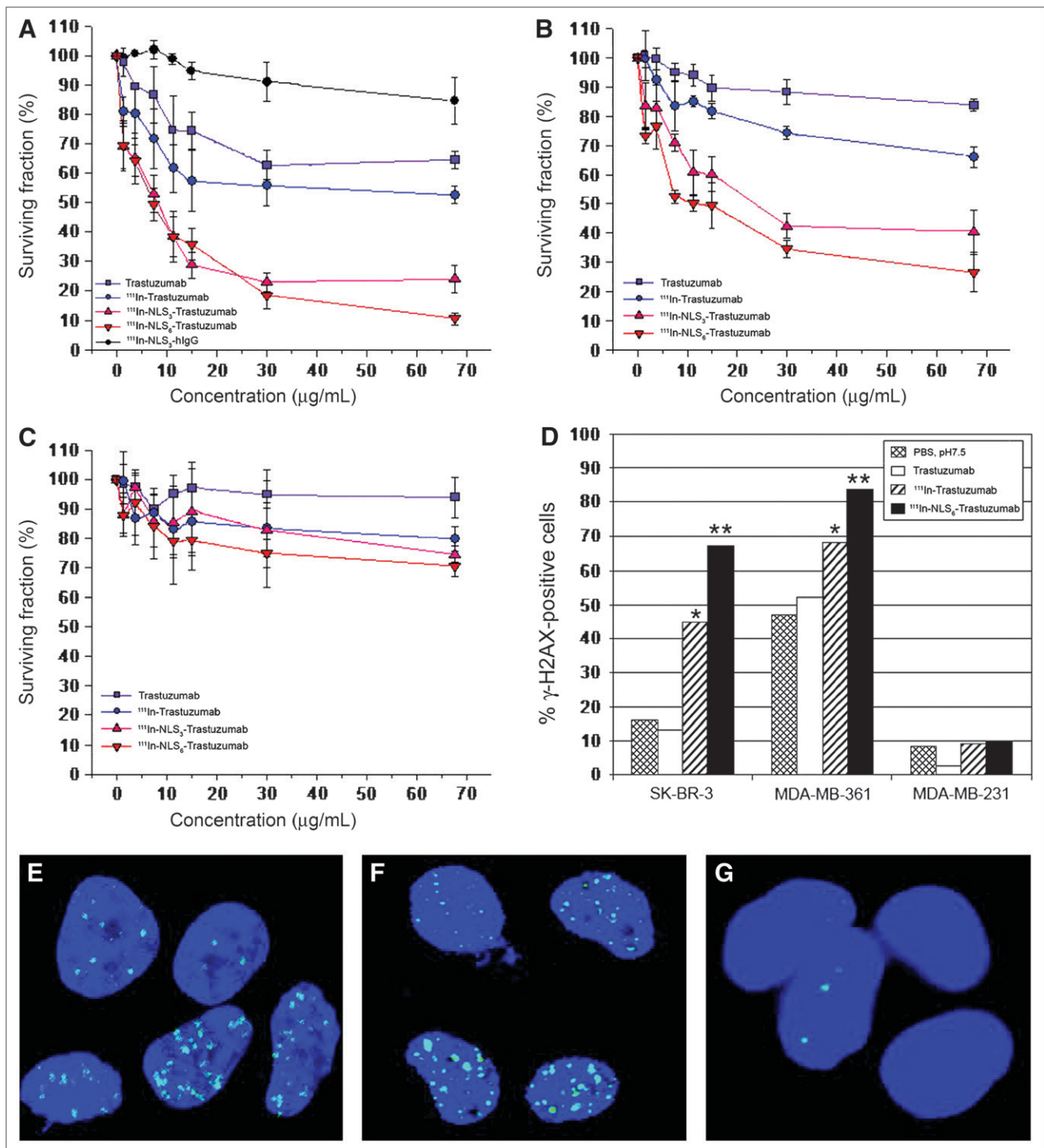


FIGURE 5. Cell survival curves measured in clonogenic assays for SK-BR-3 (A), MDA-MB-361 (B), and MDA-MB-231 (C) BC cells treated with increasing concentrations of ¹¹¹In-Trastuzumab, ¹¹¹In-NLS₃-Trastuzumab, or ¹¹¹In-NLS₆-Trastuzumab. Controls consisted of cells treated with unlabeled trastuzumab or irrelevant ¹¹¹In-NLS₃-IgG. Each point represents mean ± SEM of 3 experiments performed in triplicate. (D) Percentage of cells positive for DNA damage (>10 γH2AX foci/cell) after treatment with PBS (pH 7.5), unlabeled trastuzumab, ¹¹¹In-Trastuzumab, or ¹¹¹In-NLS₆-Trastuzumab. Significant differences are **P* < 0.05, ¹¹¹In-Trastuzumab compared with unlabeled trastuzumab and ***P* < 0.05, ¹¹¹In-NLS₆-Trastuzumab compared with ¹¹¹In-Trastuzumab. (E–G) Induction of γH2AX foci (green) in SK-BR-3 (E), MDA-MB-361(F), and MDA-MB-231 (G) cells after ¹¹¹In-NLS₆-Trastuzumab treatment. Nuclear DNA was stained with DAPI (blue).

TABLE 1
Tumor and Normal Tissue Uptake in MDA-MB-361 Tumor-Bearing Mice 72 Hours After Intravenous Injection

Tissue	¹¹¹ In-Trastuzumab	¹¹¹ In-NLS ₃ -Trastuzumab	¹¹¹ In-NLS ₆ -Trastuzumab	¹¹¹ In-NLS ₃ -hIgG
Blood	2.30 ± 0.37	2.31 ± 0.48	2.20 ± 0.12	3.18 ± 0.51
Bladder	2.81 ± 0.53	2.26 ± 0.37	2.37 ± 0.22	3.83 ± 0.66
Large intestine	1.59 ± 0.13	1.20 ± 0.21	1.26 ± 0.07	1.36 ± 0.09
Small intestine	2.44 ± 0.21	1.87 ± 0.21	1.91 ± 0.16	2.05 ± 0.15
Stomach	1.06 ± 0.10	0.89 ± 0.16	0.84 ± 0.12	0.99 ± 0.10
Spleen	7.17 ± 0.47	6.68 ± 0.83	7.05 ± 1.08	7.13 ± 0.61
Liver	11.46 ± 0.51	11.02 ± 0.37	12.27 ± 0.41	12.60 ± 0.91
Kidney	7.95 ± 0.53	7.70 ± 0.80	8.01 ± 0.26	8.23 ± 0.84
Lung	3.20 ± 0.21	2.64 ± 0.33	2.81 ± 0.05	3.63 ± 0.33
Heart	2.35 ± 0.26	2.08 ± 0.37	2.27 ± 0.13	2.54 ± 0.33
Muscle	1.37 ± 0.18	1.03 ± 0.22	0.90 ± 0.07	1.33 ± 0.26
Skin	2.11 ± 0.21	2.10 ± 0.50	2.05 ± 0.20	2.90 ± 0.38
Bone marrow	2.73 ± 0.71	2.92 ± 0.12	2.68 ± 0.28	3.33 ± 0.54
Tumor	13.17 ± 2.22 ^a	12.14 ± 1.34 ^b	12.62 ± 0.44 ^c	4.78 ± 0.76 ^d

a-d, b-d, c-d Significantly different.

a-b, a-c, b-c Not significantly different.

Statistical comparisons between groups were made by Student *t* test (*P* < 0.05). Results are expressed as mean %ID/g ± SEM (*n* = 6, except bone marrow, where *n* = 3).

NLS-enhanced but HER2/neu receptor-mediated internalization of ¹¹¹In-trastuzumab is unknown. However, Ginj et al. similarly reported a 3.6-fold higher receptor-mediated uptake of an ¹¹¹In-labeled somatostatin-based conjugate in AR4-2J rat pancreatic acinar tumor cells when modified with the NLS of SV40 large-T antigen (29). It has been suggested that cationic macromolecules rapidly undergo endocytosis via an absorptive-mediated process through binding to negatively charged cell-surface proteins (32). Although the SV40 NLS-peptides used in our study possess several cationic lysine residues, the uptake of radioactivity by SK-BR-3 cells exposed to ¹¹¹In-NLS-trastuzumab was blocked by unlabeled trastuzumab, demonstrating that internalization was HER2/neu-mediated. Ginj et al. (29) showed that unconjugated ¹¹¹In-aminohexyl-DOTA-*PKKKRKV* peptides harboring the same SV40 large T-antigen NLS (italicized) as that in the NLS-peptides (CGYG*PKKKRKV*GG) used in our study were not bound or internalized by AR4-2J tumor cells or SSTR_{2A}-expressing HEK-293 cells.

There were no significant differences in tumor uptake and tumor-to-blood ratios for ¹¹¹In-NLS-trastuzumab and ¹¹¹In-trastuzumab in MDA-MB-361 xenograft-bearing mice, but these were significantly higher than those for ¹¹¹In-NLS-hIgG—nonspecific, irrelevant control immunoconjugates, thus demonstrating that tumor uptake was HER2/neu-specific (Table 1). Normal tissue uptake was comparable with that reported for ¹¹¹In-trastuzumab in mice bearing SK-OV-3 human ovarian cancer xenografts (33). Thus, the NLS-peptides did not affect the biodistribution properties of ¹¹¹In-trastuzumab but did promote HER2/neu-specific nuclear uptake in vivo in MDA-MB-361 BC xenografts (Table 2). In contrast, no differences in nuclear uptake between ¹¹¹In-trastuzumab and ¹¹¹In-NLS-trastuzumab were found in cells isolated from the liver, spleen, kidneys, and heart, which may be attributable to the fact that trastuzumab recognizes only human HER2/neu (33); the inability to cross-recognize mouse C-erbB-2 would preclude receptor-mediated internalization of ¹¹¹In-NLS-trastuzumab into

TABLE 2
In Vivo Nuclear Uptake in MDA-MB-361 Tumor-Bearing Mice 72 Hours After Intravenous Injection

Tissue	¹¹¹ In-Trastuzumab	¹¹¹ In-NLS ₃ -Trastuzumab	¹¹¹ In-NLS ₆ -Trastuzumab	¹¹¹ In-NLS ₃ -hIgG
Liver	0.78 ± 0.17	1.11 ± 0.30	1.14 ± 0.35	1.21 ± 0.30
Kidney	0.80 ± 0.28	1.16 ± 0.13	1.00 ± 0.35	1.14 ± 0.24
Spleen	0.51 ± 0.22	0.85 ± 0.13	1.08 ± 0.05	0.87 ± 0.22
Heart	0.15 ± 0.02	0.12 ± 0.04	0.15 ± 0.07	0.11 ± 0.02
Tumor	1.13 ± 0.32 ^a	2.42 ± 0.24 ^b	2.89 ± 0.35 ^c	0.48 ± 0.08 ^d

a-b, a-c, b-d, c-d Significantly different.

a-d, b-c Not significantly different.

Statistical comparisons between groups were made by Student *t* test (*P* < 0.05). Results are expressed as mean %ID/g ± SEM (*n* = 3).

TABLE 3
Radiation-Absorbed Dose Estimates to Cell Nucleus by ¹¹¹In-NLS-Trastuzumab Localized in Compartments of MDA-MB-361 Human Breast Cancer Cell*

Cell compartment	\bar{A}^\dagger (Bq × s)	S [(Gy/Bq × s) × 10 ⁻⁴]	Radiation dose to cell nucleus D [‡] (Gy)
Membrane	14,500	1.78	2.58
Cytoplasm	2,100	3.18	0.67
Nucleus	4,100	60.30	24.72
		Total	27.97

*Cellular radiation dosimetry model of Goddu et al. (34) was used to estimate radiation-absorbed dose (D) to cell nucleus: $D = \bar{A} \times S$, where S is radiation-absorbed dose in nucleus (Gy) per unit of cumulated radioactivity in source compartment, \bar{A} (Bq × s).

[†]Assumes rapid localization of ¹¹¹In-NLS-trastuzumab in compartment and rate of elimination corresponding to radioactive decay of radionuclide, ¹¹¹In. $\bar{A} = A_0/\lambda$, where A_0 is amount of radioactivity localized in compartment at time 0 and λ is radioactive decay constant for ¹¹¹In ($2.83 \times 10^{-6}/s$).

[‡]Based on targeting a MDA-MB-361 human BC cell with diameter of 10 μm and nucleus with diameter of 6 μm to receptor saturation with ¹¹¹In-NLS-trastuzumab. At concentrations of radioligand leading to receptor saturation, ~60 mBq ¹¹¹In-NLS-trastuzumab would be bound to each MDA-MB-361 cell at specific activity of 3.6×10^{10} MBq/mol.

these cells, although there remains the possibility of Fc-mediated internalization by hepatocytes or splenocytes.

Microdosimetry estimates to the nucleus of a single MDA-MB-361 cell (1×10^6 HER2/neu receptors/cell) from exposure to ¹¹¹In-NLS-trastuzumab (specific activity, 240 MBq/mg; 3.6×10^{10} MBq/mol) at receptor-saturation conditions were calculated using the method of Goddu et al. (34) (Table 3) on the basis of the following assumptions: (a) the compartmental distribution in the cells was 70% bound to the membrane, 10% in the cytoplasm, and 20% in the nucleus based on the results of the internalization and nuclear fractionation experiments (Fig. 3; Table 2); (b) the diameters of the cell and nucleus were 10 and 6 μm, respectively; and (c) there was elimination from these compartments only by radioactive decay. The microdosimetry estimates revealed that ¹¹¹In-NLS-trastuzumab could potentially deliver as much as 27.9 Gy to the nucleus of a MDA-MB-361 cell. These radiation-absorbed doses are 1.4-fold higher than those reported by us for MDA-MB-468 cells (19.3 Gy) for ¹¹¹In-DTPA-hEGF, an Auger electron-emitting radiotherapeutic agent for metastatic BC overexpressing epidermal growth factor receptor (19). Furthermore, they reveal that the 20% of radioactivity imported into the nucleus of a MDA-MB-361 cell accounts for approximately 90% of the total radiation-absorbed dose to the nucleus. Higher doses could potentially be delivered to SK-BR-3 cells (2×10^6 HER2/neu receptors/cell), whereas lower doses would be deposited in MDA-MB-231 cells that express a 150-fold lower level of HER2/neu (18).

CONCLUSION

We conclude that NLS-peptides efficiently routed ¹¹¹In-trastuzumab to the nucleus of HER2/neu-positive human BC cells, where the nanometer–micrometer Auger electrons rendered the radiotherapeutic agent damaging to DNA and lethal to the cells. The efficacy of ¹¹¹In-NLS-trastuzumab for eradicating cultured HER2/neu-overexpressing BC cells

in vitro and its favorable tumor-targeting properties in vivo warrant future radioimmunotherapeutic studies in mice to evaluate its antitumor properties and normal tissue toxicities.

ACKNOWLEDGMENTS

This research was supported by grants from the Canadian Breast Cancer Research Alliance (grant 016456) with funds from the Canadian Cancer Society, the Canadian Breast Cancer Foundation (Ontario Chapter), the Connaught Fund, and the Leslie Dan Faculty of Pharmacy. D.L.C. and Z.C. are Canadian Institutes of Health Research Strategic Training Fellows in the Excellence in Radiation Research for the 21st Century (EIRR21) Program. The authors acknowledge the contribution of April Eryou in conducting initial studies of this work. Parts of this manuscript were presented at the European Symposium on Radiopharmacy and Radiopharmaceuticals in Lucca, Italy, March 30–April 2, 2006.

REFERENCES

1. Wu AM, Senter PD. Arming antibodies: prospects and challenges for immunoconjugates. *Nat Biotechnol.* 2005;23:1137–1146.
2. Slamon DJ, Leyland-Jones B, Shak S, et al. Use of chemotherapy plus a monoclonal antibody against HER2 for metastatic breast cancer that overexpresses HER2. *N Engl J Med.* 2001;344:783–792.
3. Cobleigh MA, Vogel CL, Tripathy D, et al. Multinational study of the efficacy and safety of humanized anti-HER2 monoclonal antibody in women who have HER2-overexpressing metastatic breast cancer that has progressed after chemotherapy for metastatic disease. *J Clin Oncol.* 1999;17:2639–2648.
4. Vogel CL, Cobleigh MA, Tripathy D, et al. Efficacy and safety of trastuzumab as a single agent in first-line treatment of HER2-overexpressing metastatic breast cancer. *J Clin Oncol.* 2002;20:719–726.
5. De Santes K, Slamon D, Anderson SK, et al. Radiolabeled antibody targeting of the HER-2/neu oncoprotein. *Cancer Res.* 1992;52:1916–1923.
6. Tsai SW, Sun Y, Williams LE, Raubitschek AA, Wu AM, Shively JE. Biodistribution and radioimmunotherapy of human breast cancer xenografts with radiometal-labeled DOTA conjugated anti-HER2/neu antibody 4D5. *Bioconjug Chem.* 2000;11:327–334.
7. Li G, Wang Y, Huang K, Zhang H, Peng W, Zhang C. The experimental study on the radioimmunotherapy of the nasopharyngeal carcinoma overexpressing HER2/neu in nude mice model with intratumoral injection of ¹⁸⁸Re-herceptin. *Nucl Med Biol.* 2005;32:59–65.

8. Milenic DE, Garmestani K, Brady ED, et al. Alpha-particle radioimmunotherapy of disseminated peritoneal disease using a ^{212}Pb -labeled radioimmunoconjugate targeting HER2. *Cancer Biother Radiopharm*. 2005;20:557–568.
9. Li Y, Cozzi PJ, Qu CF, et al. Cytotoxicity of human prostate cancer cell lines in vitro and induction of apoptosis using ^{213}Bi -Herceptin alpha-conjugate. *Cancer Lett*. 2004;205:161–171.
10. Akabani G, Carlin S, Welsh P, Zalutsky MR. In vitro cytotoxicity of ^{211}At -labeled trastuzumab in human breast cancer cell lines: effect of specific activity and HER2 receptor heterogeneity on survival fraction. *Nucl Med Biol*. 2006;33:333–347.
11. Ballangrud AM, Yang WH, Palm S, et al. Alpha-particle emitting atomic generator (actinium-225)-labeled trastuzumab (Herceptin) targeting of breast cancer spheroids: efficacy versus HER2/neu expression. *Clin Cancer Res*. 2004;10:4489–4497.
12. Buchegger F, Perillo-Adamer F, Dupertuis YM, Delaloye AB. Auger radiation targeted into DNA: a therapy perspective. *Eur J Nucl Med Mol Imaging*. 2006;33:1352–1363.
13. Miederer M, McDevitt MR, Sgouros G, Kramer K, Cheung NK, Scheinberg DA. Pharmacokinetics, dosimetry, and toxicity of the targetable atomic generator, ^{225}Ac -HuM195, in nonhuman primates. *J Nucl Med*. 2004;45:129–137.
14. Boswell CA, Brechbiel MW. Auger electrons: lethal, low energy, and coming soon to a tumor cell nucleus near you. *J Nucl Med*. 2005;46:1946–1947.
15. Yoneda Y, Semba T, Kaneda Y, et al. A long synthetic peptide containing a nuclear localization signal and its flanking sequences of SV40 T-antigen directs the transport of IgM into the nucleus efficiently. *Exp Cell Res*. 1992;201:313–320.
16. Chen P, Wang J, Hope K, et al. Nuclear localizing sequences promote nuclear translocation and enhance the radiotoxicity of the anti-CD33 monoclonal antibody HuM195 labeled with ^{111}In in human myeloid leukemia cells. *J Nucl Med*. 2006;47:827–836.
17. Tang Y, Wang J, Scollard DA, et al. Imaging of HER2/neu-positive BT-474 human breast cancer xenografts in athymic mice using ^{111}In -trastuzumab (Herceptin) Fab fragments. *Nucl Med Biol*. 2005;32:51–58.
18. Konecny G, Pauletti G, Pegram M, et al. Quantitative association between HER2/neu and steroid hormone receptors in hormone receptor-positive primary breast cancer. *J Natl Cancer Inst*. 2003;95:142–153.
19. Reilly RM, Kiarash R, Cameron RG, et al. ^{111}In -Labeled EGF is selectively radiotoxic to human breast cancer cells overexpressing EGFR. *J Nucl Med*. 2000;41:429–438.
20. Peng M, Litman R, Jin Z, Fong G, Cantor SB. BACH1 is a DNA repair protein supporting BRCA1 damage response. *Oncogene*. 2006;25:2245–2253.
21. Hu M, Chen P, Wang J, Chan C, Scollard DA, Reilly RM. Site-specific conjugation of HIV-1 tat peptides to IgG: a potential route to construct radioimmunoconjugates for targeting intracellular and nuclear epitopes in cancer. *Eur J Nucl Med Mol Imaging*. 2006;33:301–310.
22. Hnatowich DJ, Childs RL, Lanteigne D, Najafi A. The preparation of DTPA-coupled antibodies radiolabeled with metallic radionuclides: an improved method. *J Immunol Methods*. 1983;65:147–157.
23. Tubbs RR, Pettay JD, Roche PC, Stoler MH, Jenkins RB, Grogan TM. Discrepancies in clinical laboratory testing of eligibility for trastuzumab therapy: apparent immunohistochemical false-positives do not get the message. *J Clin Oncol*. 2001;19:2714–2721.
24. Cardoso F, Piccart MJ, Durbecq V, Di Leo A. Resistance to trastuzumab: a necessary evil or a temporary challenge? *Clin Breast Cancer*. 2002;3:247–257; discussion, 258–249.
25. Michel RB, Andrews PM, Castillo ME, Mattes MJ. In vitro cytotoxicity of carcinoma cells with ^{111}In -labeled antibodies to HER-2. *Mol Cancer Ther*. 2005;4:927–937.
26. Howell RW. Radiation spectra for Auger-electron emitting radionuclides: report no. 2 of AAPM Nuclear Medicine Task Group no. 6. *Med Phys*. 1992;19:1371–1383.
27. Wasielewski M, Elstrodt F, Klijn JG, Berns EM, Schutte M. Thirteen new p53 gene mutants identified among 41 human breast cancer cell lines. *Breast Cancer Res Treat*. 2006;99:97–101.
28. Austin CD, De Maziere AM, Pisacane PI, et al. Endocytosis and sorting of ErbB2 and the site of action of cancer therapeutics trastuzumab and geldanamycin. *Mol Biol Cell*. 2004;15:5268–5282.
29. Ginj M, Hinni K, Tschumi S, Schulz S, Maecke HR. Trifunctional somatostatin-based derivatives designed for targeted radiotherapy using Auger electron emitters. *J Nucl Med*. 2005;46:2097–2103.
30. Haefliger P, Agorastos N, Renard A, Giambonini-Brugnoli G, Marty C, Alberto R. Cell uptake and radiotoxicity studies of an nuclear localization signal peptide-intercalator conjugate labeled with $^{99\text{m}}\text{Tc}(\text{CO})_3^+$. *Bioconjug Chem*. 2005;16:582–587.
31. Ong GL, Mattes MJ. Limitations in the use of low pH extraction to distinguish internalized from cell surface-bound radiolabeled antibody. *Nucl Med Biol*. 2000;27:571–575.
32. Pardridge WM, Buciak J, Yang J, Wu D. Enhanced endocytosis in cultured human breast carcinoma cells and in vivo biodistribution in rats of a humanized monoclonal antibody after cationization of the protein. *J Pharmacol Exp Ther*. 1998;286:548–554.
33. Lub-de Hooge MN, Kosterink JG, Perik PJ, et al. Preclinical characterisation of ^{111}In -DTPA-trastuzumab. *Br J Pharmacol*. 2004;143:99–106.
34. Goddu SM, Howell RW, Rao DV. Cellular dosimetry: absorbed fractions for monoenergetic electron and alpha particle sources and S-values for radionuclides uniformly distributed in different cell compartments. *J Nucl Med*. 1994;35:303–316.